IEEE Access
Multidisciplinary | Rapid Review | Open Access Journal

Received February 27, 2020, accepted March 14, 2020, date of publication March 17, 2020, date of current version March 26, 2020.

Digital Object Identifier 10.1109/ACCESS.2020.2981479

An Improved Beam Training Scheme Under Hierarchical Codebook

HONGKANG YU, PENGXIN GUAN, WANYUE QU, AND YUPING ZHAO
School of Electronics Engineering and Computer Science, Peking University, Beijing 100871, China
Corresponding author: Yuping Zhao (yuping.zhao@pku.edu.cn)

ABSTRACT In millimeter wave (mmWave) communications, the beamforming gains of large-scale antenna arrays are used to combat severe path losses and improve communication link quality. This requires beam training (BT) to determine the optimal beam direction and achieve beam alignment. The hierarchical codebook with multi-resolution training beams is widely used in BT to reduce training overhead. Unfortunately, due to hardware restrictions, the transition area between two adjacent training beams often leads to error propagation in a traditional BT scheme, which limits the accuracy of beam alignment. In this paper, we propose an improved BT scheme under hierarchical codebook. First, we define an index to measure the power difference of the received signals. Once the index is lower than the predefined threshold, the optimal beam direction is considered to be in the transition area, and an extra interval that contains the transition area is proposed for further beam searching. Then, we analyze the optimal threshold and the probability of beam misalignment based on the ideal beam pattern, proving that the error rate exponentially decreases with the signal-to-noise ratio (SNR) under a single-path channel with constant gain. Finally, simulation results demonstrate that the proposed scheme can significantly improve the accuracy of beam alignment and is applicable to most existing beam patterns.

INDEX TERMS Hierarchical codebook, millimeter wave, beam training, beam alignment, error propagation, beam alignment error rate.

I. INTRODUCTION

Millimeter wave (mmWave) communication is regarded as one of the most promising technologies for future wireless communication systems, and its abundant spectrum resources can significantly increase system capacity [1], [2]. However, due to severe path losses in the mmWave band, the beamforming gains of large-scale antenna arrays are required to increase communication distances [3]–[5]. Since mmWave beams with high gain are usually very narrow, it is important to align the beams of the transmitter and the receiver. The accuracy of beam alignment has a significant influence on the link quality and communication reliability [6], [7].

In a frequency division duplex (FDD) system, a transmitter cannot acquire the channel state information through channel reciprocity. Beam training (BT) is a common approach used to realize beam alignment [7]–[18]. During BT, the transmitter sends training beams with different spatial angles, which are selected from a predefined codebook. Then, the optimal beam direction is obtained through receiver feedback. One typical BT method uses an exhaustive search, where the transmitter sends all training beams in the codebook to cover the entire search range and then selects the best beam [8]–[10]. However, this method requires excessive training overhead, which limits its application.

To reduce training overhead, a multi-resolution hierarchical codebook architecture is widely used in BT [11]–[18]. The hierarchical codebook consists of multiple layers, which correspond to multiple training stages. The transmitter starts by sending wide beams of the first layer, which covers the whole search range. By processing the received signals, a reduced search range is determined for the next training stage. As BT is performed layer by layer, the training beams of each successive layer become narrower. Finally, a beam with a specific resolution is obtained through this divide-and-conquer strategy.

Existing studies on hierarchical codebooks have mainly focused on beam pattern design. In [11], the deactivation (DEACT) antenna processing technique is used to control the beam width, which is only realized by analog devices such as phase shifters. Moreover, [12]–[16] depend on a subarray architecture of hybrid beamforming, designing the beam

The associate editor coordinating the review of this manuscript and approving it for publication was Emrecan Demirors.

patterns through the cooperation of subarrays. The hardware implementation of these two categories is relatively simple, but a certain gap exists between the designed beam patterns and the ideal one. For example, the designed beams usually have a large ripple, which is adverse to beam alignment and user fairness. To address this problem, more accurate training beams are designed based on the full-connection architecture of hybrid beamforming [17], [18]. In [17], a least squares method is proposed. Similarly, a beam pattern shaping approach (BPSA) is introduced in [18], which formulates the beam design as a convex optimization problem. With the help of a more complex hardware structure, these methods effectively reduce the ripple of the beam, and achieve better performance.

It should be noted that the studies mentioned above use the same BT scheme and only differ in the beam pattern. In these studies, once the search interval is determined with error in a certain BT stage, each following stage will search in the wrong area. This manifests as the error propagation problem in the traditional BT scheme, which limits the accuracy of beam alignment. To the best of our knowledge, this problem attracts little attention. Literature [18] points out that the transition band of the training beams has an influence on error propagation. It proposes to modify the main lobe of the beam to cover the transition band of the previous layer, which can help reduce error propagation. However, this method results in a reduction of the beam gain, as well as the beam resolution. More importantly, it relies heavily on the design of narrow transition bands, and is not suitable for pure analog beamforming and subarray architecture.

In this paper, we focus on BT scheme under hierarchical codebook instead of beam pattern design. To address error propagation, we propose an improved BT scheme. The contributions are summarized as follows:

- We propose an index to measure the power difference of the received signals and compares the index with a predefined threshold. When the index is greater, we determine the search interval in the same way as the traditional BT scheme. Otherwise, we define an extra search interval in the next training stage, which overlaps with the traditional one.
- We analyze the performance of the proposed method theoretically. Based on the ideal beam pattern, the approximate expression of the optimal threshold and the beam alignment error probability (BAER) are derived. The BAER of the proposed scheme exponentially decreases with the signal-to-noise ratio (SNR) under a single-path channel with constant gain, which provides a considerable advantage over the traditional scheme where the BAER shows a linear decline.
- Simulation results in the mmWave channel also show that the proposed scheme can significantly reduce BAER and does not depend on specific hardware implementation, which provides flexibility in practice.

The rest of this paper is organized as follows. Section II introduces the system model, gives a brief review of the hierarchical codebook and the traditional BT scheme. In Section III, the improved BT scheme under hierarchical codebook is proposed. Section IV analyzes the performance of the proposed scheme theoretically. Section V presents the simulation results. Section VI concludes the paper.

Notation: a, $\mathbf{a}$, $\mathbf{A}$ and $\mathcal{A}$ denote a scalar variable, a vector, a matrix and a set, respectively. $(\cdot)^{\mathrm{T}}$ and $(\cdot)^{\mathrm{H}}$ denote transpose and conjugate transpose, respectively. $|\cdot|$ and $\|\cdot\|$ denote absolute value and 2-norm, respectively. $\mathcal{CN}(\mu, \sigma^2)$ and $\mathcal{N}(\mu, \sigma^2)$ represent complex and real Gaussian random variable with mean μ and variance σ^2, respectively. $\mathrm{Re}\{\cdot\}$ and $\mathrm{Im}\{\cdot\}$ denote the real and imaginary part of a complex number, respectively. In addition, $\Phi(x)$ represents the cumulative distribution function (CDF) of normal distribution, $\mathrm{erf}(x)$ and $\mathrm{erfc}(x)$ represent error function and complementary error function, respectively. $\circ$ represents entry-wise product.

II. SYSTEM MODEL AND REVIEW OF PRIOR WORK

A. SYSTEM SETUP

A point-to-point multiple-input single-output (MISO) system is considered in this paper, where the transmitter has N_t antennas. We assume that the receiver has only one antenna for simplicity, as the proposed BT scheme can be extended to the multi-antenna receiver easily. Since we consider the mmWave channel, the widely used Saleh-Valenzuela channel model with Rician fading is adopted [10], [16], where the channel vector is considered to be the sum of line of sight (LoS) and non-LoS (NLoS) components. For the NLoS component, we assume that it consists of L paths. Furthermore, a uniform linear antenna array is deployed at the transmitter, such that the channel vector can be expressed as

$$\mathbf{h} = \alpha_0 \mathbf{a}(\phi_0) + \sqrt{\frac{1}{L}} \sum_{i=1}^{L} \alpha_i \mathbf{a}(\phi_i), \tag{1}$$

where $\mathbf{a}(\phi) = \frac{1}{\sqrt{N_t}}[1, e^{j\frac{2\pi}{\lambda}d\phi}, \ldots, e^{j\frac{2\pi}{\lambda}(N_t-1)d\phi}]^{\mathrm{T}}$ represents the array response vector, α_0 and α_i are complex gains of the LoS and NLoS paths, respectively. The parameter ϕ_i is the cosine value of the physical angle of departure (AoD) φ_i, i.e., $\phi_i = \cos\varphi_i \in [-1, 1]$. For convenience, the AoD means its cosine value in the next section.

To obtain a higher beamforming gain, the BT scheme needs to estimate the strongest multi-path component, i.e., the AoD of the LoS component ϕ_0. Therefore, the unit-power pilot signal x is processed by the beamforming vector $\mathbf{w}$, which is selected from the predefined codebook at the transmitter side. Thus, the received signal can be expressed as

$$y = \sqrt{\rho}\mathbf{h}^{\mathrm{H}}\mathbf{w}x + n, \tag{2}$$

where ρ denotes the normalized transmitted power, $\|\mathbf{w}\| = 1$ and $n \sim \mathcal{CN}(0, 1)$ is the normalized noise. It should be noted that the proposed BT method does not specify the specific implementation for the beamforming vector $\mathbf{w}$. It may be a pure analog beamforming vector or be realized by the hybrid beamforming structure. By processing the received signals

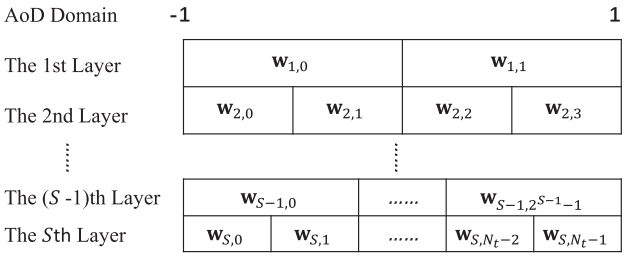

FIGURE 1. An illustration of a multi-resolution hierarchical codebook.

from the different training beams, the receiver can obtain an estimate of ϕ_0 and feed the result back to the transmitter.

B. HIERARCHICAL CODEBOOK

To reduce the training overhead, the hierarchical codebook is widely used in BT [11]–[18]. As shown in Fig. 1, the hierarchical codebook is divided into $S = \log_2 N_t$ layers, which correspond to different BT stages. We assume N_t is a dyadic integer without loss of generality. There are a total of 2^s codewords in the sth layer, corresponding to training beams with different directions. Beams of the same layer have the same width

$$w_s = 2^{1-s}, \tag{3}$$

dividing the entire search interval into 2^s portions. This implies that the training beams of the higher layer are narrower. Moreover, the hierarchical codebook specifies that the beam coverage of the $(s-1)$th layer is covered by a pair of beams of the sth layer. Mathematically, the coverage of the bth beam of the sth layer $\mathbf{w}_{s,b}$ is given by

$$\mathcal{I}_{s,b} = [-1 + bw_s, -1 + (b+1)\, w_s], \quad \text{for} \quad s \in \{1, \ldots, S\}, b \in \{0, \ldots, 2^s - 1\}. \tag{4}$$

The beam coverage of two adjacent layers satisfies $\mathcal{I}_{s-1,b} = \mathcal{I}_{s,2b} \cup \mathcal{I}_{s,2b+1}$.

In the traditional BT scheme, the transmitter sends the pilot signal beamformed by the vectors $\mathbf{w}_{1,0}$ and $\mathbf{w}_{1,1}$ during the first training stage. The receiver obtains corresponding signals $y_{1,0}$ and $y_{1,1}$. If $y_{1,0} > y_{1,1}$, the reduced search interval is determined as $\mathcal{I}_{1,0}$; otherwise, $\mathcal{I}_{1,1}$ is used for a further search. The receiver tells the transmitter result via 1-bit feedback. In the next stage, two narrower training beams of the second layer are transmitted, which cover the newly determined search interval. As BT continues layer by layer, the search interval of the AoD shrinks. Finally, $\hat{\phi}_0$ is obtained as an estimate of ϕ_0 at layer S. The detailed process is summarized in Algorithm 1.

Ideally, when the SNR condition is good and the LoS component is strong enough, the desired beam alignment accuracy of the traditional BT scheme is $1/N$, i.e., $\left|\phi_0 - \hat{\phi}_0\right| \leq 1/N$. However, due to hardware limitations, a transition band between the main lobe and the side lobe of the beam always exists. The traditional BT scheme only compares the power of the received signals to determine the search interval. As a result, when the AoD is located in the transition band, the power of the two adjacent training beams is close, which leads to detection error on a certain layer [18]. Once the wrong AoD search interval is determined, the search interval of the following layers and the final estimate will be wrong. This manifests as the error propagation problem in the hierarchical codebook. To address this problem, we propose an improved BT scheme in the next section.

Algorithm 1 Traditional BT Scheme

Input: codebook layers S, hierarchical codebook $\mathbf{w}_{s,b}$
Output: aligned beam direction $\hat{\phi}_0$

```
Initialize: m = 0;
for s = 1 to S do
    The transmitter sends pilot signals beamformed by w_{s,m} and w_{s,m+1};
    The receiver obtains corresponding signals y_{s,0} and y_{s,1}, compares their power and tells the transmitter through 1-bit feedback;
    if |y_{s,0}|^2 < |y_{s,1}|^2 then
        m := 2m
    end if
end for
φ̂_0 := −1 + (m+1)/2^S
```

III. IMPROVED BEAM TRAINING SCHEME

For almost all the beam patterns designed under the hierarchical codebook, the beamforming gains of two adjacent beams are close in the transition band, which is the main cause of error propagation in the traditional BT scheme. Additionally, we notice that the difference in the beamforming gains at the main lobe is much larger. This inspired us to judge whether the AoD is located in the transition band according to the power difference of the received signals. If the power difference is small, the AoD is considered to be in the transition band. In the next training stage, this area will be searched exclusively. Otherwise, the search interval is determined in the same way as the traditional BT scheme.

We use Fig. 2 as an illustration of the proposed BT scheme. First, we redefine the expression of the search interval. As seen from Fig. 2(a), we assume that the search interval of the sth training stage is $[\phi^s, \phi^s + 2w_s]$, where w_s denotes the beam width and is consistent with (3) in the traditional method. Thus, the search interval in each stage is uniquely determined by the starting point ϕ^s. The transmitter sends two beams $\mathbf{w}_{s,0}^{\phi^s}$ and $\mathbf{w}_{s,1}^{\phi^s}$, and their coverages are denoted as $\mathcal{I}_s^{\phi^s} = [\phi^s, \phi^s + w_s]$ and $\mathcal{I}_s^{\phi^s + w_s} = [\phi^s + w_s, \phi^s + 2w_s]$, respectively. According to [12], [18], $\mathbf{w}_{s,0}^{\phi^s}$ and $\mathbf{w}_{s,1}^{\phi^s}$ can be determined by a phase rotation factor, which can be expressed as

$$\mathbf{w}_{s,i}^{\phi^s} = \mathbf{w}_{s,i} \circ \sqrt{N_t}\mathbf{a}\left(\phi^s + 1\right), i \in \{0, 1\}, \tag{5}$$

where $\mathbf{w}_{s,i}$ denotes the ith beam of the sth layer in the hierarchical codebook.

When the receiver obtains the training signals, it calculates the difference in power and compares it with a predefined

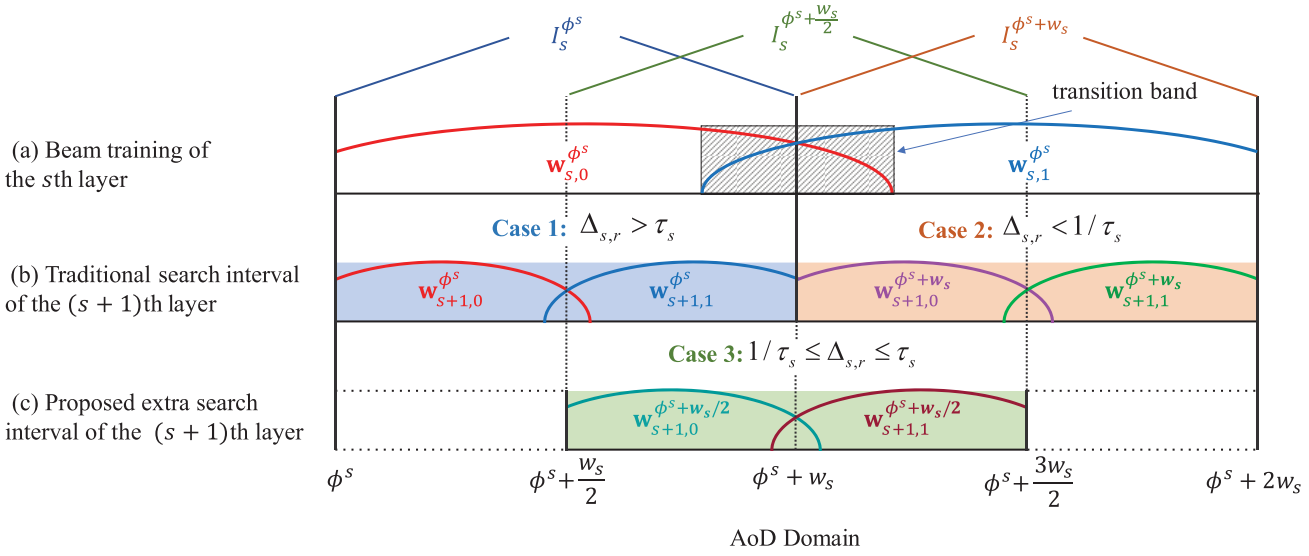

FIGURE 2. An illustration of the proposed beam training scheme and its search interval.

threshold τ_s. For example, we can take $\Delta_{s,r} = |y_{s,0}|^2/|y_{s,1}|^2$ as an index to measure the power difference. Based on the relationship between $\Delta_{s,r}$ and τ_s, there are three possible search intervals to be determined in the next training stage. If $\Delta_{s,r} > \tau_s$, we determine the search interval as $\mathcal{I}_s^{\phi^s}$. Similarly, if $\Delta_{s,r} < 1/\tau_s$, i.e., $|y_{s,1}|^2/|y_{s,0}|^2 > \tau_s$, $\mathcal{I}_s^{\phi^s+w_s}$ is determined for a further search. These two cases are shown in Fig. 2(b), which is similar to the traditional BT scheme. The largest difference is that once the values of $|y_{s,0}|^2$ and $|y_{s,1}|^2$ are close, i.e., $1/\tau_s \le \Delta_{s,r} \le \tau_s$, the AoD is considered to be in the transition band. To ensure compatibility with the hierarchical codebook, we adjust the search interval to $\mathcal{I}_s^{\phi^s+w_s/2}$, which has the same width as the traditional search interval and covers the transition band, as shown in Fig. 2(c). Since $\mathcal{I}_s^{\phi^s+w_s/2}$ overlaps with $\mathcal{I}_s^{\phi^s}$ and $\mathcal{I}_s^{\phi^s+w_s}$, we designate the proposed method as beam training with overlapping interval (BTOI). The starting angle of the search interval under BTOI can be summarized as

$$\phi^{s+1} = \begin{cases} \phi^s, & \Delta_{s,r} > \tau_s \\ \phi^s + \dfrac{w_s}{2}, & \dfrac{1}{\tau_s} \le \Delta_{s,r} \le \tau_s \\ \phi^s + w_s, & \Delta_{s,r} < \dfrac{1}{\tau_s} \end{cases} \tag{6}$$

In the same way, we can also use the difference of the power $\Delta_{s,d} = |y_{s,0}|^2 - |y_{s,1}|^2$ as an index to measure the power difference. The corresponding detection method is

$$\phi^{s+1} = \begin{cases} \phi^s, & \Delta_{s,d} > \tau_s \\ \phi^s + \dfrac{w_s}{2}, & -\tau_s \le \Delta_{s,d} \le \tau_s \\ \phi^s + w_s, & \Delta_{s,d} < -\tau_s \end{cases} \tag{7}$$

In BTOI, the value of τ_s has a significant impact on system performance. Obviously, the traditional BT scheme can be regarded as a special case of BTOI for $\tau_{s,r} = 1$ (ratio index) or $\tau_{s,d} = 0$ (difference index). To obtain the optimal threshold under different beam patterns and different channel conditions, an offline Monte Carlo (MC) simulation method is used. Then the optimal threshold is applied in the real scenario. Specifically, we optimize for conditional error probability p_s, which represents the probability of beam misalignment in the sth training stage given that the previous search intervals are all correctly detected [18]. By setting different threshold values $\tau_{s,i}$, the corresponding $p_s(\tau_{s,i})$ are obtained by simulation, such that the optimal threshold value can be determined as $\tau_s^* = \arg\min_i p_s(\tau_{s,i})$. The complete BTOI process is summarized in Algorithm 2.

Algorithm 2 BTOI

Input: codebook layers S, hierarchical codebook $\mathbf{w}_{s,b}$, predefined threshold τ_s

Output: aligned beam direction $\hat{\phi}_0$

1: Initialize: $\phi^1 = -1$;
2: **for** $s = 1$ to S **do**
3: The transmitter sends pilot signals beamformed by $\mathbf{w}_{s,0}^{\phi^s}$ and $\mathbf{w}_{s,1}^{\phi^s}$ according to (5);
4: The receiver obtains corresponding signals $y_{s,0}$ and $y_{s,1}$, calculates $\Delta_{s,d}$ or $\Delta_{s,r}$, compares it with τ_s and tells the transmitter through 2-bit feedback;
5: The transmitter determines ϕ^{s+1} according to (6) or (7);
6: **end for**
7: $\hat{\phi}_0 := \phi^{S+1} + \frac{1}{2^S}$

Compared with the traditional BT scheme, BTOI can fully discover the information carried by the received power. By setting the extra search interval $\mathcal{I}_s^{\phi^s+w_s/2}$, BTOI can significantly reduce error propagation when the AoD is located in the transition area. We provide a theoretical analysis in the next section. Meanwhile, the width of the search interval under BTOI is the same as the traditional method. As a result,

most existing beam patterns can be extended to BTOI easily. Finally, the extra process at the receiver only includes the calculation of the power difference, and an additional bit is required at each training stage to feedback three possible situations. Thus, the proposed scheme requires only slight increases in both time complexity and training overhead.

IV. THEORETICAL ANALYSIS OF BTOI SCHEME

In this section, we theoretically analyze the optimal threshold and the BAER. Similar to [9], [18], [19], for tractability, we focus the analysis on a single-path channel. We assume that the channel gain is constant, which is suitable when the LoS component is deterministic [10]. The effects of random fading and the NLoS component are shown by the simulation method.

Since BTOI determines the AoD search interval based on the power difference, the CDF of Δ_s is required for performance analysis. We take the distribution of the difference value $\Delta_{s,d}$ as an example. According to [18], the power of the received signal obeys a non-central chi-squared distribution with 2 degrees of freedom, which causes the CDF of $\Delta_{s,d}$ to be too complex. Thus, we first present an approximate probability distribution of $\Delta_{s,d}$.

Proposition 1: For a certain AoD $\phi \in [\phi^s, \phi^s + 2w_s]$, assume that $\mathbf{h} = \mathbf{a}(\phi)$, and the received powers of noise-free signals under two training beams are $\lambda_{s,0}(\phi) = \rho\left|\mathbf{a}^{\mathrm{H}}(\phi)\mathbf{w}_{s,0}^{\phi^s}\right|^2$ and $\lambda_{s,1}(\phi) = \rho\left|\mathbf{a}^{\mathrm{H}}(\phi)\mathbf{w}_{s,1}^{\phi^s}\right|^2$, respectively. The random variable $\Delta_{s,d}$ can be approximated as Gaussian distribution with a mean of $\mu_s(\phi) = \lambda_{s,0}(\phi) - \lambda_{s,1}(\phi)$ and a variance of $\sigma_s^2(\phi) = 2\left(\lambda_{s,0}(\phi) + \lambda_{s,1}(\phi)\right)$.

Proof: See Appendix A. ∎

According to Proposition 1, the CDF of $\Delta_{s,d}$ under AoD ϕ can be approximated as $\mathrm{F}(\tau;\phi) = \Phi\left(\frac{\tau-\mu_s(\phi)}{\sigma_s(\phi)}\right)$, which helps us calculate the probability of beam misalignment. For example, we consider the sth training stage and assume that ϕ is located in $[0, w_s/2]$. According to (7), a detection error occurs if $\Delta_{s,d} < \tau_s$ and the probability is $\mathrm{F}(\tau_s;\phi)$. To derive the conditional error probability, we assume ϕ distributes uniformly in $[0, 2w_s]$ without loss of generality. Then the full expression of p_s can be calculated as (8), as shown at the bottom of this page. Considering the symmetry of the beam patterns about w_s, we have $\mathrm{F}(\tau_s;\phi) = 1 - \mathrm{F}(-\tau_s; 2w_s - \phi)$ for $\phi \in [0, w_s]$. Thus, equation (8) can be simplified as

$$p_s(\tau_s) = \frac{1}{w_s}\left(\int_0^{w_s/2} \mathrm{F}(\tau_s;\phi)d\phi + \int_{w_s/2}^{w_s} \mathrm{F}(-\tau_s;\phi)d\phi\right). \tag{10}$$

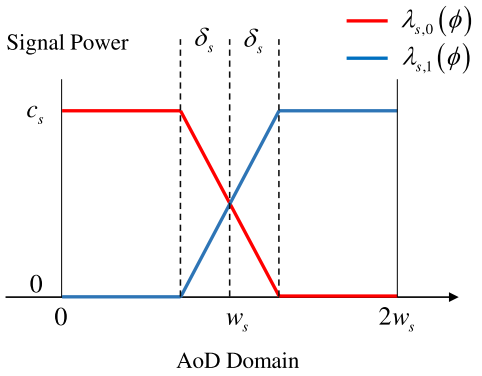

FIGURE 3. Diagram of the ideal beam pattern with a transition band.

Next, we derive the optimal threshold theoretically. Considering the diversity of the beam patterns under different hardware implementations, and the integral term in (10) is difficult to handle, we focus on the ideal beam pattern with a transition band, as illustrated in Fig. 3. Assuming that the gain of a unit-power ideal beam is g_s in the main lobe, then the values of $\lambda_{s,0}$ and $\lambda_{s,1}$ are $c_s = \rho g_s$ in the main lobe. Meanwhile, the values in the side lobe are 0. We also assume that the beam gain changes linearly in the transition band, and the width of the transition band is $2\delta_s$, such that $\mu_s(\phi) = -\frac{c_s}{\delta_s}\phi + \frac{c_s w_s}{\delta_s}$ in $[w_s - \delta_s, w_s + \delta_s]$. According to the characteristics of the ideal beam pattern, by omitting the subscript, equation (10) can be transformed into (9), as shown at the bottom of this page, where (a) is obtained by $\Phi(x) = \frac{1}{2}\left[1 + \mathrm{erf}\left(x/\sqrt{2}\right)\right]$ and $\mathrm{erf}(x) = -\mathrm{erf}(-x)$, (b) is obtained from $g(x) = \int \mathrm{erf}(x)\,dx = x\mathrm{erf}(x) + \frac{1}{\sqrt{\pi}}e^{-x^2}$ [20].

To obtain the optimal threshold, the derivative of $p(\tau)$ is derived as

$$p'(\tau) = \frac{1}{4\sqrt{\pi c}}e^{-\frac{(c-\tau)^2}{4c}} - \left(0.5 - \frac{\delta}{w}\right)\frac{1}{2\sqrt{\pi c}}e^{-\frac{(-c-\tau)^2}{4c}} - \frac{\delta}{2cw}\left(\mathrm{erf}\left(\frac{c+\tau}{2\sqrt{c}}\right) - \mathrm{erf}\left(\frac{\tau}{2\sqrt{c}}\right)\right), \tag{11}$$

$$p_s(\tau_s) = \frac{1}{2w_s}\left(\int_0^{w_s/2} \mathrm{F}(\tau_s;\phi)d\phi + \int_{w_s/2}^{w_s} \mathrm{F}(-\tau_s;\phi)d\phi + \int_{w_s}^{3w_s/2} (1 - \mathrm{F}(\tau_s;\phi))\,d\phi + \int_{3w_s/2}^{2w_s} (1 - \mathrm{F}(-\tau_s;\phi))\,d\phi\right) \tag{8}$$

$$\begin{aligned} p(\tau) &= 0.5\Phi\left(\frac{\tau - c}{\sqrt{2c}}\right) + \left(0.5 - \frac{\delta}{w}\right)\Phi\left(\frac{-\tau - c}{\sqrt{2c}}\right) + \frac{1}{w}\int_0^{\delta} \Phi\left(\frac{-\frac{c}{\delta}t - \tau}{\sqrt{2c}}\right)dt \\ &\overset{(a)}{=} 0.5\Phi\left(\frac{\tau - c}{\sqrt{2c}}\right) + \left(0.5 - \frac{\delta}{w}\right)\Phi\left(\frac{-\tau - c}{\sqrt{2c}}\right) + \frac{\delta}{2w} - \frac{1}{2w}\int_0^{\delta} \mathrm{erf}\left(\frac{\frac{c}{\delta}t + \tau}{2\sqrt{c}}\right)dt \\ &\overset{(b)}{=} 0.5\Phi\left(\frac{\tau - c}{\sqrt{2c}}\right) + \left(0.5 - \frac{\delta}{w}\right)\Phi\left(\frac{-\tau - c}{\sqrt{2c}}\right) + \frac{\delta}{2w} - \frac{\delta}{\sqrt{c}w}\left(g\left(\frac{\tau + c}{2\sqrt{c}}\right) - g\left(\frac{\tau}{2\sqrt{c}}\right)\right) \end{aligned} \tag{9}$$

where we use $\Phi'(x) = \frac{1}{\sqrt{2\pi}}e^{-x^2/2}$ and $\mathrm{erf}'(x) = \frac{2}{\sqrt{\pi}}e^{-x^2}$. We also derive the second derivative of $p(\tau)$, which can be expressed as

$$p''(\tau) = \frac{c-\tau}{8c\sqrt{\pi c}}e^{-\frac{(c-\tau)^2}{4c}} + \left(0.5 - \frac{\delta}{w}\right)\frac{c+\tau}{4c\sqrt{\pi c}}e^{-\frac{(c+\tau)^2}{4c}} + \frac{\delta}{2cw\sqrt{\pi c}}\left(e^{-\frac{\tau^2}{4c}} - e^{-\frac{(c+\tau)^2}{4c}}\right). \quad (12)$$

Obviously, $p''(\tau) > 0$ for $\tau \in (0, c)$, which implies $p(\tau)$ is convex in $(0, c)$. Moreover, it is easy to verify that $p'(0) < 0$ and $p'(c) > 0$. Thus, the optimal threshold $\tau^* \in (0, c)$ exists to minimize $p(\tau)$, which can be obtained by solving $p'(\tau^*) = 0$ through the numerical method.

To further study the BAER of BTOI under the optimal threshold, we derive an approximation of the optimal threshold under high SNR conditions.[1]

Proposition 2: Under the condition of high SNR, τ^* can be approximated as

$$\tau_s^* \approx \frac{\rho g_s}{2} - \ln \rho g_s + 2\ln\frac{\delta_s\sqrt{\pi}}{3w_s}. \quad (13)$$

Proof: See Appendix B. ■

According to Proposition 2, the optimal threshold is not fixed, but changes dynamically with the SNR. When the SNR is high, the optimal threshold for the ideal beam pattern can be set to half of the main lobe beam gain. With the optimal threshold, the BAER of BTOI can be approximated as [18]

$$P_{\mathrm{BTOI}} = \mathbb{P}\left(\left|\phi_0 - \hat{\phi}_0\right| \le \frac{1}{N}\right) \approx 1 - \prod_s \left(1 - p_s\left(\tau_s^*\right)\right). \quad (14)$$

To further demonstrate the performance gain of BTOI over the traditional BT scheme, we analyze the asymptotic characteristics of the two schemes in the high SNR regime.

Proposition 3: Under the condition of high SNR, the BAER of the traditional BT scheme under the ideal beam pattern can be approximated as

$$P_{\mathrm{traditional}} \approx \frac{1}{\sqrt{\rho\pi}}\sum_s \frac{\delta_s}{\sqrt{g_s w_s}}. \quad (15)$$

The BAER of BTOI can be approximately bounded by

$$P_{\mathrm{BTOI}} \lessapprox \frac{1}{24}\left(1 - \frac{\delta_1}{w_1}\right)e^{-\frac{1}{16}\rho g_1}. \quad (16)$$

Proof: See Appendix C. ■

From Proposition 3, we find that the BAER of the traditional BT scheme decreases linearly with the SNR in the log-log coordinate. It should be noted that a similar conclusion is proposed in [19], but we complete the proof from a novel perspective of the ideal beam pattern. We also prove that the offset of the BAER curve is determined by the ratio of the transition band width to the beam width. For BTOI, we find that the BAER decreases exponentially with the SNR in the log-log coordinate, which demonstrates a considerable advantage over the traditional BT scheme.

[1] In practice, enough power should be allocated during the training stage. The SNR can be increased by sending beams repeatedly [15], [18]. Moreover, simulation result shows that it is also consistent with theoretical BAER under low SNR conditions.

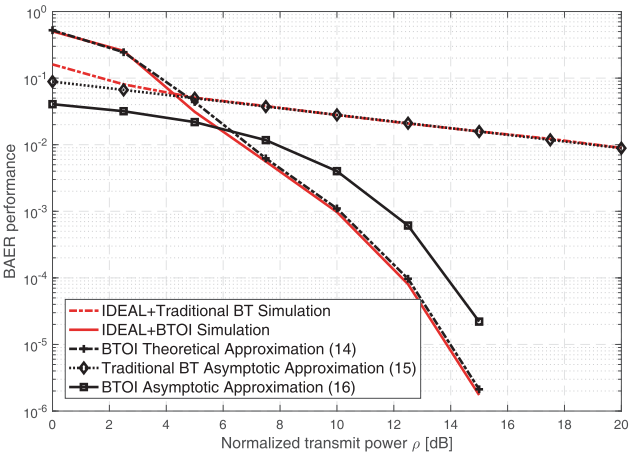

FIGURE 4. BAER performance and theoretical analysis for the ideal beam pattern under the traditional BT scheme and the proposed BTOI.

V. SIMULATION RESULTS

In this section, simulation results are presented to demonstrate the performance of BTOI and compare it with the traditional BT scheme. In the simulation, we set $N_t = 64$, $S = 6$, $d = 0.5\lambda$. We also assume that ϕ_i distributes uniformly in $[-1, 1]$. To verify that BTOI is applicable to beam patterns under different hardware architectures, the DEACT codebook in [11], the beam widening via single-RF subarray (BMWSS) codebook in [12], and the BPSA codebook in [18] are selected. We observe the BAER performance improvement under BTOI combined with these codebooks.

Since our analysis is based on a single-path channel with constant gain, we first set the simulation parameters as $\alpha_0 = 1$ and $L = 0$. Fig. 4 verifies the theoretical analysis of the ideal beam pattern and compares the BAER performance of the traditional BT scheme and BTOI. The determination of g_s and δ_s for the ideal beam pattern refers to the BPSA codebook, and the threshold is obtained according to (13). As shown in the figure, when the SNR is low, the performance of BTOI is not as good as that of the traditional BT scheme. This is mainly because of the gap between the approximate optimal threshold and the actual threshold under low SNR conditions. As the SNR increases, the BAER of BTOI decreases rapidly, which is much better than the traditional method. Meanwhile, we observe that the theoretical BAER of BTOI calculated by (14) is consistent with the simulation result, confirming the correctness of the theoretical derivation. Finally, we observe that the asymptotic approximation of BAER under the traditional BT scheme agrees with the simulation result in the high SNR regime, which demonstrates a linear decline. For BTOI, one can observe that the upper bound provided by Proposition 3 is effective but not tight, mainly because the threshold is set to $c_s/2$ rather than the optimal value. However, we can see the same exponential downward trend of the

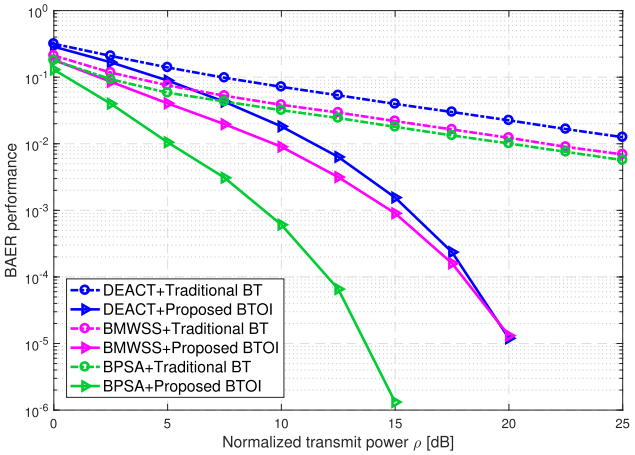

FIGURE 5. BAER performance for three different beam patterns on a single-path channel under the traditional BT scheme and the proposed BTOI.

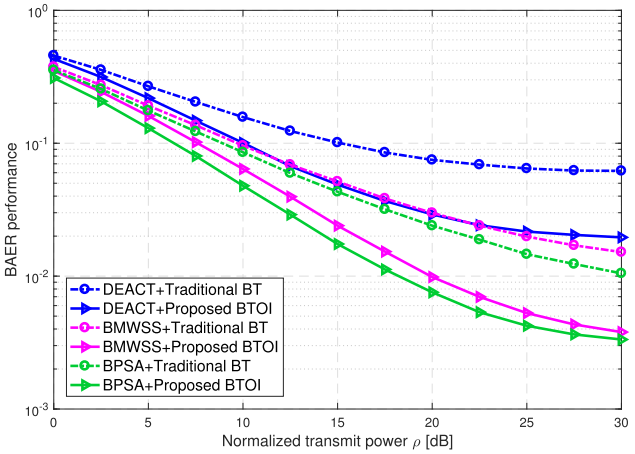

FIGURE 6. BAER performance for three different beam patterns on a multi-path mmWave channel under the traditional BT scheme and the proposed BTOI.

simulation result, which provides a theoretical guarantee for the advantage of BTOI.

Fig. 5 shows the BAER performance of three different beam patterns on a single-path channel under the traditional BT scheme and BTOI. We take the difference value $\Delta_{s,d}$ as an index to measure the power difference, and the thresholds are determined by the offline MC simulation method. We can see that BTOI outperforms the traditional BT scheme under all three beam patterns in the whole SNR regime. The BAER curve for the traditional BT scheme decreases linearly as the SNR increases, while the BAER of BTOI degrades rapidly, which is consistent with the theoretical analysis.

Next, we consider the BAER performance on a multi-path mmWave channel. We set the channel with $L = 3$, $\alpha_0 \sim \mathcal{CN}(0,1)$ and $\alpha_i \sim \mathcal{CN}(0, 10^{-1})$. Fig. 6 compares the performance of the traditional BT scheme and BTOI. Here we use the ratio value $\Delta_{s,r}$ as an index to measure the power difference and obtain the threshold through MC simulation. Due to the influence of channel fading and the NLoS component, the BAER performance degrades compared to the single-path channel, but BTOI still maintains the BAER improvement over the traditional BT scheme. Additionally, this improvement does not depend on the beam patterns and is applicable to different hardware architectures.

VI. CONCLUSION

This paper studies the error propagation problem in the hierarchical codebook. We propose an improved BT scheme named BTOI. Different from the traditional scheme that only compares the power of the received signals to determine the search interval of the next training stage, BTOI calculates the power difference and compares it with a predefined threshold. Moreover, an extra special search interval including the transition band is designed, which helps reduce the detection error when the AoD is located in the transition area. We analyze the performance of BTOI, proving that the BAER decreases exponentially with the SNR, which shows a considerable advantage compared with the traditional scheme, where the error rate decreases linearly. Simulation results show that BTOI outperforms the traditional BT scheme from the perspective of BAER and is applicable to most existing beam patterns.

APPENDIXES

APPENDIX A
PROOF OF PROPOSITION 1

The received power in the sth training stage can be expressed as

$$\begin{aligned}|y_{s,i}|^2 &= \left|\sqrt{\rho}\mathbf{a}^{\mathrm{H}}(\phi)\mathbf{w}_{s,i}^{\phi^s} + n_i\right|^2 \\ &= \left(\mathrm{Re}\left\{\sqrt{\rho}\mathbf{a}^{\mathrm{H}}(\phi)\mathbf{w}_{s,i}^{\phi^s}\right\} + \mathrm{Re}\{n_i\}\right)^2 \\ &\quad + \left(\mathrm{Im}\left\{\sqrt{\rho}\mathbf{a}^{\mathrm{H}}(\phi)\mathbf{w}_{s,i}^{\phi^s}\right\} + \mathrm{Im}\{n_i\}\right)^2, i \in \{0,1\}. \end{aligned} \tag{17}$$

Let $z_{i,0} = \mathrm{Re}\left\{\sqrt{\rho}\mathbf{a}^{\mathrm{H}}(\phi)\mathbf{w}_{s,i}^{\phi^s}\right\}$, $z_{i,1} = \mathrm{Im}\left\{\sqrt{\rho}\mathbf{a}^{\mathrm{H}}(\phi)\mathbf{w}_{s,i}^{\phi^s}\right\}$, $n_{i,0} = \mathrm{Re}\{n_i\}$, $n_{i,1} = \mathrm{Im}\{n_i\}$, $\Delta_{s,d}$ can be expressed as

$$\begin{aligned}\Delta_{s,d} &= |y_{s,0}|^2 - |y_{s,1}|^2 \\ &= \lambda_{s,0} - \lambda_{s,1} + 2z_{0,0}n_{0,0} + 2z_{0,1}n_{0,1} \\ &\quad - 2z_{1,0}n_{1,0} - 2z_{1,1}n_{1,1} \\ &\quad + n_{0,0}^2 + n_{0,1}^2 - n_{1,0}^2 - n_{1,1}^2. \end{aligned} \tag{18}$$

When the SNR is high, we can ignore the influence of the last four terms in (18). Since $n_i \sim \mathcal{CN}(0,1)$, $n_{i,0}$ and $n_{i,1}$ are independent and follow Gaussian distribution with $\mathcal{N}(0, 0.5)$. Therefore, $\Delta_{s,d}$ can be seen as a Gaussian variable approximately. Obviously, it has the mean of $\lambda_{s,0} - \lambda_{s,1}$, and the variance is calculated by

$$\begin{aligned}\sigma_s^2 &= 0.5 \times 4\left(z_{0,0}^2 + z_{0,1}^2 + z_{1,0}^2 + z_{1,1}^2\right) \\ &= 2\left(\lambda_{s,0} + \lambda_{s,1}\right), \end{aligned} \tag{22}$$

so the proposition is proved.

$$p'(\tau) \approx \frac{1}{4\sqrt{\pi c}} e^{-\frac{(c-\tau)^2}{4c}} - \left(0.5 - \frac{\delta}{w}\right) \frac{1}{2\sqrt{\pi c}} e^{-\frac{(c+\tau)^2}{4c}} - \frac{\delta}{12cw}\left(e^{-\frac{\tau^2}{4c}} - e^{-\frac{(c+\tau)^2}{4c}}\right) - \frac{\delta}{4cw}\left(e^{-\frac{\tau^2}{3c}} - e^{-\frac{(c+\tau)^2}{3c}}\right) \tag{19}$$

$$\begin{aligned} p(0) &= \left(1 - \frac{\delta}{w}\right)\Phi\left(-\sqrt{\frac{c}{2}}\right) + \frac{\delta}{2w} - \frac{\delta}{\sqrt{c}w}\left(g\left(\frac{\sqrt{c}}{2}\right) - g(0)\right) \\ &= \frac{1}{2}\left(1 - \frac{\delta}{w}\right)\left(1 + \mathrm{erf}\left(-\frac{\sqrt{c}}{2}\right)\right) + \frac{\delta}{2w} - \frac{\delta}{\sqrt{c}w}\left(\frac{\sqrt{c}}{2}\mathrm{erf}\left(\frac{\sqrt{c}}{2}\right) + \frac{1}{\sqrt{\pi}}e^{-\frac{c}{4}} - \frac{1}{\sqrt{\pi}}\right) \\ &= \frac{1}{2}\mathrm{erfc}\left(\frac{\sqrt{c}}{2}\right) - \frac{\delta}{\sqrt{c\pi}w}e^{-\frac{c}{4}} + \frac{\delta}{\sqrt{c\pi}w} \\ &\approx \frac{\delta}{\sqrt{c\pi}w} \end{aligned} \tag{20}$$

$$\begin{aligned} p\left(\frac{c}{2}\right) &= 0.5\Phi\left(-\frac{\sqrt{c}}{2\sqrt{2}}\right) + \left(0.5 - \frac{\delta}{w}\right)\Phi\left(-\frac{3\sqrt{c}}{2\sqrt{2}}\right) + \frac{\delta}{2w} - \frac{\delta}{\sqrt{c}w}\left(g\left(\frac{3\sqrt{c}}{4}\right) - g\left(\frac{\sqrt{c}}{4}\right)\right) \\ &= \frac{w+\delta}{4w} + \mathrm{erfc}\left(\frac{3\sqrt{c}}{4}\right) + \frac{w-\delta}{4w}\mathrm{erfc}\left(\frac{\sqrt{c}}{4}\right) - \frac{\delta}{\sqrt{c\pi}w}\left(e^{-\frac{9}{16}c} - e^{-\frac{1}{16}c}\right) \\ &\approx \frac{w+\delta}{4w}\left(\frac{1}{6}e^{-\frac{9}{16}c} + \frac{1}{2}e^{-\frac{3}{4}c}\right) + \frac{w-\delta}{4w}\left(\frac{1}{6}e^{-\frac{1}{16}c} + \frac{1}{2}e^{-\frac{1}{12}c}\right) - \frac{\delta}{\sqrt{c\pi}w}\left(e^{-\frac{9}{16}c} - e^{-\frac{1}{16}c}\right) \\ &\approx \left(\frac{1}{24} - \frac{\delta}{24w} + \frac{\delta}{\sqrt{c\pi}w}\right)e^{-\frac{1}{16}c} \\ &\approx \frac{1}{24}\left(1 - \frac{\delta}{w}\right)e^{-\frac{1}{16}c} \end{aligned} \tag{21}$$

APPENDIX B
PROOF OF PROPOSITION 2

First, we derive the approximate expression of (11). Since $\mathrm{erf}(x) = 1 - \mathrm{erfc}(x)$, we use $\mathrm{erfc}(x)$ instead of $\mathrm{erf}(x)$. Then, according to [21], $\mathrm{erfc}(x)$ can be approximated at $x > 0$ as

$$\mathrm{erfc}(x) \approx \frac{1}{6}e^{-x^2} + \frac{1}{2}e^{-\frac{4}{3}x^2}. \tag{23}$$

Thus, (11) can be approximated as (19), as shown at the top of this page.

When the SNR is high, the value of c is large, which obviously corresponds to a large threshold value. Thus, we can ignore the higher-order terms and obtain

$$p'(\tau) \approx \frac{1}{4\sqrt{\pi c}} e^{-\frac{(c-\tau)^2}{4c}} - \frac{\delta}{12cw} e^{-\frac{\tau^2}{4c}}. \tag{24}$$

Let the derivative be 0, then we obtain (13), and the proposition is proved.

APPENDIX C
PROOF OF PROPOSITION 3

For the traditional BT scheme, we substitute $\tau = 0$ into (9) to obtain the conditional error probability (20), as shown at the top of this page, where we use $\Phi(x) = \frac{1}{2}\left(1 + \mathrm{erf}\left(\frac{x}{\sqrt{2}}\right)\right)$, $\mathrm{erf}(x) = -\mathrm{erf}(-x)$ and $\mathrm{erf}(x) = 1 - \mathrm{erfc}(x)$. The last step uses (23) and omits higher-order terms. According to [18], the BAER can be approximated as $\sum_s p_s(\tau)$, so we can obtain (15).

For BTOI, we substitute $\tau = c/2$ into (9). Using a similar derivation mentioned above, we can obtain (21), as shown at the top of this page. Since the beam gain of the first layer is the lowest compared to other layers, it has the most important impact on the BAER, and we use p_1 to approximate P_{BTOI}. Since $c/2$ is not the optimal threshold, (16) is derived as an approximate upper bound of the BAER.

REFERENCES

[1] T. S. Rappaport, S. Sun, R. Mayzus, H. Zhao, Y. Azar, K. Wang, G. N. Wong, J. K. Schulz, M. Samimi, and F. Gutierrez, "Millimeter wave mobile communications for 5G cellular: It will work!," *IEEE Access*, vol. 1, pp. 335–349, 2013.

[2] W. Roh, J.-Y. Seol, J. Park, B. Lee, J. Lee, Y. Kim, J. Cho, K. Cheun, and F. Aryanfar, "Millimeter-wave beamforming as an enabling technology for 5G cellular communications: Theoretical feasibility and prototype results," *IEEE Commun. Mag.*, vol. 52, no. 2, pp. 106–113, Feb. 2014.

[3] T. S. Rappaport, F. Gutierrez, E. Ben-Dor, J. N. Murdock, Y. Qiao, and J. I. Tamir, "Broadband millimeter-wave propagation measurements and models using adaptive-beam antennas for outdoor urban cellular communications," *IEEE Trans. Antennas Propag.*, vol. 61, no. 4, pp. 1850–1859, Apr. 2013.

[4] R. W. Heath, N. Gonzalez-Prelcic, S. Rangan, W. Roh, and A. M. Sayeed, "An overview of signal processing techniques for millimeter wave MIMO systems," *IEEE J. Sel. Topics Signal Process.*, vol. 10, no. 3, pp. 436–453, Apr. 2016.

[5] T. L. Marzetta, "Noncooperative cellular wireless with unlimited numbers of base station antennas," *IEEE Trans. Wireless Commun.*, vol. 9, no. 11, pp. 3590–3600, Nov. 2010.

[6] E. Onggosanusi, M. S. Rahman, L. Guo, Y. Kwak, H. Noh, Y. Kim, S. Faxer, M. Harrison, M. Frenne, S. Grant, R. Chen, R. Tamrakar, and A. Q. Gao, "Modular and high-resolution channel state information and beam management for 5G new radio," *IEEE Commun. Mag.*, vol. 56, no. 3, pp. 48–55, Mar. 2018.

[7] V. W. S. Wong, R. Schober, D. W. K. Ng, and L.-C. Wang, *Key Technologies for 5G Wireless Systems*. Cambridge, U.K.: Cambridge Univ. Press, 2017.

[8] C. Jeong, J. Park, and H. Yu, "Random access in millimeter-wave beamforming cellular networks: Issues and approaches," *IEEE Commun. Mag.*, vol. 53, no. 1, pp. 180–185, Jan. 2015.

[9] M. Li, C. Liu, S. V. Hanly, I. B. Collings, and P. Whiting, "Explore and eliminate: Optimized two-stage search for millimeter-wave beam alignment," *IEEE Trans. Wireless Commun.*, vol. 18, no. 9, pp. 4379–4393, Sep. 2019.
[10] L. Zhao, D. W. K. Ng, and J. Yuan, "Multi-user precoding and channel estimation for hybrid millimeter wave systems," *IEEE J. Sel. Areas Commun.*, vol. 35, no. 7, pp. 1576–1590, Jul. 2017.
[11] T. He and Z. Xiao, "Suboptimal beam search algorithm and codebook design for millimeter-wave communications," *Mobile Netw. Appl.*, vol. 20, no. 1, pp. 86–97, Feb. 2015.
[12] Z. Xiao, T. He, P. Xia, and X.-G. Xia, "Hierarchical codebook design for beamforming training in millimeter-wave communication," *IEEE Trans. Wireless Commun.*, vol. 15, no. 5, pp. 3380–3392, May 2016.
[13] R. Zhang, H. Zhang, W. Xu, and X. You, "Subarray-cooperation-based multi-resolution codebook and beam alignment design for mmWave backhaul links," *IEEE Access*, vol. 7, pp. 18319–18331, 2019.
[14] Z. Xiao, P. Xia, and X.-G. Xia, "Channel estimation and hybrid precoding for millimeter-wave MIMO systems: A low-complexity overall solution," *IEEE Access*, vol. 5, pp. 16100–16110, 2017.
[15] S. Noh, M. D. Zoltowski, and D. J. Love, "Multi-resolution codebook based beamforming sequence design in millimeter-wave systems," in *Proc. IEEE Global Commun. Conf. (GLOBECOM)*, Dec. 2015, pp. 1–6.
[16] R. Zhang, H. Zhang, W. Xu, and X. You, "Subarray-based simultaneous beam training for multiuser mmWave massive MIMO systems," *IEEE Wireless Commun. Lett.*, vol. 8, no. 4, pp. 976–979, Aug. 2019.
[17] A. Alkhateeb, O. El Ayach, G. Leus, and R. W. Heath, Jr., "Channel estimation and hybrid precoding for millimeter wave cellular systems," *IEEE J. Sel. Topics Signal Process.*, vol. 8, no. 5, pp. 831–846, Oct. 2014.
[18] J. Zhang, Y. Huang, Q. Shi, J. Wang, and L. Yang, "Codebook design for beam alignment in millimeter wave communication systems," *IEEE Trans. Commun.*, vol. 65, no. 11, pp. 4980–4995, Nov. 2017.
[19] C. Liu, M. Li, S. V. Hanly, I. B. Collings, and P. Whiting, "Millimeter wave beam alignment: Large deviations analysis and design insights," *IEEE J. Sel. Areas Commun.*, vol. 35, no. 7, pp. 1619–1631, Jul. 2017.
[20] E. W. Ng and M. Geller, "A table of integrals of the error functions," *J. Res. Nat. Bur. Standards B*, vol. 73, no. 1, pp. 1–20, 1969.
[21] M. Chiani, D. Dardari, and M. K. Simon, "New exponential bounds and approximations for the computation of error probability in fading channels," *IEEE Trans. Wireless Commun.*, vol. 24, no. 5, pp. 840–845, May 2003.

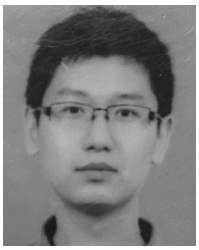

HONGKANG YU received the B.E. degree in communication engineering from Beijing Jiaotong University, China, in 2016. He is currently pursuing the Ph.D. degree in information and communication engineering with the School of Electronics Engineering and Computer Science, Peking University, China. In 2016, he was a Laboratory Engineer with the Institute of Wireless Communication and Signal Processing. His current research interests include millimeter wave, massive MIMO, and channel estimation.

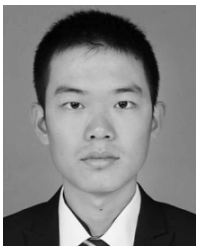

PENGXIN GUAN received the B.E. degree in communication engineering from the University of Science and Technology Beijing, China, in 2018. He is currently pursuing the Ph.D. degree in information and communication engineering with the School of Electronics Engineering and Computer Science, Peking University, China. In 2018, he was a Laboratory Engineer with the Institute of Wireless Communication and Signal Processing. His current research interests include the Internet of Things, full-duplex wireless communications, and signal processing in wireless communications.

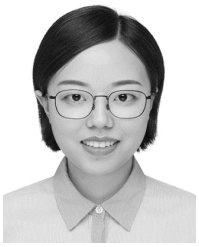

WANYUE QU received the B.E. degree in communication engineering from Xidian University, China, in 2014. She is currently pursuing the Ph.D. degree in information and communication engineering with the School of Electronics Engineering and Computer Science, Peking University, China. In 2014, she was a Laboratory Engineer with the Institute of Wireless Communication and Signal Processing. Her current research interests include multiple-input–multiple-output systems, device-to-device, and resource allocation.

YUPING ZHAO received the B.S. and M.S. degrees in electrical engineering from Northern Jiaotong University, Beijing, China, in 1983 and 1986, respectively, and the Ph.D. and Doctor of Science degrees in wireless communications from Aalto University, Espoo, Finland, in 1997 and 1999, respectively. She was a System Engineer for telecommunication companies in China and Japan. She was a Research Engineer with the Nokia Research Center, Helsinki, Finland, in radio resource management for wireless mobile communication networks. She is currently a Professor with the State Key Laboratory of Advanced Optical Communication Systems and Networks, School of Electronics Engineering and Computer Science, Peking University, Beijing. Her current research interests include wireless communications and corresponding signal processing, especially for orthogonal frequency-division multiplexing, ultra-wideband, multiple-input–multiple-output systems, cooperative networks, cognitive radio, and wireless sensor networks.